Chemical Geology 673 (2025) 122522

Contents lists available at ScienceDirect

Chemical Geology

journal homepage: www.elsevier.com/locate/chemgeo

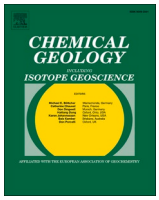

Grassland woody encroachment alters subsurface mineral weathering and groundwater composition in a carbonate system

Christa Anhold [a], Camden Hatley [a,b], Eresay Alcantar-Velasquez [a], Rachel M. Keen [c,d,e], Kayalvizhi Sadayappan [f], Karla M. Jarecke [g,h], Pamela L. Sullivan [h], Jesse B. Nippert [c], Li Li [f], G.L. Macpherson [b], Matthew F. Kirk [a,*]

[a] Department of Geology, Kansas State University, Manhattan, KS, USA
[b] Department of Geology, University of Kansas, Lawrence, KS, USA
[c] Division of Biology, Kansas State University, Manhattan, KS, USA
[d] Kansas Biological Survey and Center for Ecological Research, University of Kansas, Lawrence, KS, USA
[e] Department of Ecology and Evolutionary Biology, University of Kansas, Lawrence, KS, USA
[f] Department of Civil and Environmental Engineering, The Pennsylvania State University, University Park, PA, USA
[g] Department of Geography, University of Colorado, Boulder, CO, USA
[h] College of Earth, Ocean, and Atmospheric Sciences, Oregon State University, Corvalis, OR, USA

ARTICLE INFO

Editor: Karen Johannesson

Keywords:
Woody plant encroachment
Carbonate weathering
Soil respiration
Soil water residence time

ABSTRACT

Displacement of grasses by woody plants (woody encroachment) is occurring in grasslands worldwide. Previous studies indicate that encroachment can alter subsurface carbon dioxide (CO_2) concentrations and mineral weathering, though these impacts are still poorly understood. To address this knowledge gap, we sampled groundwater and stream water every three weeks during the 2022 water year from two watersheds at Konza Prairie Biological Station, a native tallgrass prairie underlain by limestone and mudrock units in Kansas, USA. Amounts of woody encroachment differ between the watersheds primarily because of differences in fire frequency. One watershed is burned annually and contains 6 % and 45 % woody plant coverage in its upland and riparian areas, respectively, whereas the other is burned every four years and contains 28 % and 74 % woody plant coverage, respectively. We expected to find higher CO_2 levels in the more encroached watershed, assuming the deep roots of woody plants increase inputs of CO_2 to bedrock. However, we found the opposite. Our results indicate that groundwater from a single limestone aquifer contained an average of 1.4 mM CO_2 in the less encroached watershed and 1.0 mM CO_2 in the more encroached watershed. Similarly, stream water CO_2 concentrations at the outlet of the less encroached watershed (0.25 mM) were more than twice that of the more encroached watershed (0.12 mM) on average. Despite these differences in CO_2 concentration, amounts of mineral weathering per liter of groundwater differed little between watersheds. We hypothesize that encroachment is causing differences in CO_2 concentrations between watersheds by decreasing the proportion of mineral weathering that occurs under conditions that are open with respect to CO_2 exchange. During open-system weathering, dissolved CO_2 consumed by weathering reactions can be replaced from an adjacent gas phase, allowing CO_2 concentrations to remain elevated as weathering progresses. In contrast, during closed-system weathering, CO_2 is not replaced and decreases in concentration as weathering progresses. If weathering primarily occurs under open-system conditions within the study area soils, which are unsaturated, and closed-system conditions within the underlying bedrock, where pores are more commonly saturated, then woody encroachment has the potential to decrease the proportion of open-system weathering by increasing soil permeability and thus decreasing soil water residence times. This hypothesis is consistent with our findings and implies that a shortening of soil water residence time with woody encroachment lowers the proportion of CO_2 delivered from the soil to the subsurface and creates a more aggressive weathering engine at depth and along deeper flow paths. Encroachment may also be altering soil CO_2 production and/or venting, though these possibilities require further investigation.

* Corresponding author at: KSU/Dept. of Geology, 108 Thompson Hall, Manhattan, KS 66506, USA.
E-mail address: mfkirk@ksu.edu (M.F. Kirk).

https://doi.org/10.1016/j.chemgeo.2024.122522
Received 5 August 2024; Received in revised form 20 November 2024; Accepted 27 November 2024
Available online 30 November 2024

1. Introduction

Woody encroachment, the displacement of grasses with native woody species, impacts hydrologic and biogeochemical processes in grasslands worldwide (Barger et al., 2011; Stevens et al., 2017). Previous studies have shown that woody encroachment alters soil moisture (Zou et al., 2014), catchment water budgets and recharge rates (Acharya et al., 2018; Huxman et al., 2005), runoff generation mechanisms and amounts (Keen et al., 2024; Qiao et al., 2017), the relative contributions of deeper flow paths to streams (Sadayappan et al., 2023), and stream discharge and intermittency (Dodds et al., 2023; Dodds et al., 2012; Keen et al., 2022; Zou et al., 2014). Moreover, woody encroachment alters soil carbon dioxide (CO_2) fluxes (Huxman et al., 2005; McCarron et al., 2003; Scott et al., 2006; Wen et al., 2021) and increases weathering rates in underlying bedrock (Leite et al., 2023; Wen et al., 2021). Grasslands cover about 30 % of the land surface and are responsible for about 20 % of global runoff (Dodds, 1997). Thus, understanding the hydrologic and biogeochemical impacts of woody encroachment is important for future water and land management over a large region of the terrestrial biosphere.

Woody encroachment occurs over decades (Silva et al., 2009) and is likely due to a combination of local and regional factors that favor C3 woody plants over C4 grasses (Collins et al., 2021). Higher rates of precipitation and concentrations of atmospheric CO_2 benefit woody plants relative to grasses and can thus promote woody encroachment (Briggs et al., 2005; Brunsell et al., 2017; Kgope et al., 2010). Grassland fire suppression causes encroachment because longer periods without fire allow greater recruitment and growth of woody plants (Briggs et al., 2005; Brunsell et al., 2017). Furthermore, overgrazing has driven woody encroachment in dryland regions of North America, Australia, and Africa by altering fire regimes and seed dispersal (Wilcox et al., 2022).

Woody encroachment impacts hydrologic and biogeochemical processes in part by altering watershed water budgets. Woody plants tend to transpire at greater rates than grasses (Keen et al., 2022; O'Keefe et al., 2020; Scott et al., 2006; Wang et al., 2018), which can lead to increased evapotranspiration in mesic grasslands as woody cover increases (Huxman et al., 2005; Wilcox et al., 2022). In semi-arid grasslands, encroachment can promote greater evaporation by increasing the proportion of bare soil (Huxman et al., 2005). Moreover, the canopies of woody plants can intercept incoming precipitation, decreasing how much water reaches watershed soils (Zou et al., 2015). These changes decrease soil moisture and thus contribute to decreases in groundwater recharge (Acharya et al., 2018) and streamflow (Dodds et al., 2023; Zou et al., 2014) in encroached watersheds.

In addition to altering how much water is added to soils and removed by evapotranspiration, woody encroachment also impacts the movement of water through watershed soils by altering soil permeability (Leite et al., 2020; Sullivan et al., 2019b). Woody plants tend to produce deeper and thicker roots than grasses (Canadell et al., 1996), which has been linked to increased soil saturated hydraulic conductivity and deepened water flow paths during storm events (Jarecke et al., 2024). Fine roots can reduce the permeability of soils by clogging pores, but thick roots can increase permeability by forming macropores (Lu et al., 2020; Pawlik et al., 2016). Macropores serve as preferential flow paths and can account for upwards of 70 % of the water flow through soils (Nimmo, 2021; Watson and Luxmoore, 1986). Thus, an increase in the abundance of thick roots can increase soil permeability and occurrence of preferential flow, which helps explain why encroachment can decrease surface runoff (i.e., overland flow) generation and increase the relative contribution deep groundwater to streamflow in grassland watersheds (Qiao et al., 2017; Sadayappan et al., 2023). Similarly, increased weathering of bedrock beneath encroached soils can increase bedrock porosity and permeability (Leite et al., 2023; Wen et al., 2021), which has the potential to shorten groundwater travel times and alter hydrologic connectivity between aquifers and streams (Dodds et al., 2023; Vero et al., 2018).

Causes of increased weathering in encroached areas are not fully understood. One possibility is that woody roots increase both chemical and physical weathering of bedrock by penetrating more deeply into the subsurface than grasses and widening bedrock fractures via root wedging (Leite et al., 2023). Secondly, relative to grasses, woody plant roots may release greater amounts of CO_2 and exudates, particularly in roots at deeper depths, which can serve as bedrock weathering agents and fuel for subsurface microbial populations that further generate CO_2 (Leite et al., 2023; Macpherson and Sullivan, 2019a; Wen et al., 2021). Indeed, past studies have identified soil respiration hot spots beneath encroaching tree and shrub species (Cable et al., 2012; Hibbard et al., 2001; McCulley et al., 2004). And third, encroachment could increase weathering by increasing the rate of groundwater flow through the bedrock (Brantley et al., 2017; Vero et al., 2018; Wen et al., 2021). Weathering rates tend to increase with flow rates because flow removes products from reaction sites and thus helps drive the reactions forward (Maher, 2010). Thus, if encroachment causes more rapid water flow through the shallow subsurface because of its impacts to soil and bedrock permeability, it could increase weathering (Xiao et al., 2021). However, greater transpiration by woody plants than grasses can decrease groundwater recharge in encroached areas (Acharya et al., 2018), at least during the growing season. Thus, the timing of precipitation relative to the growing season may determine the net impact of encroachment on flow.

To learn more about the potential impacts of woody encroachment on bedrock weathering, this study asks the question: how do groundwater and stream CO_2 concentrations vary between watersheds with different extents of woody encroachment? We hypothesized that the watershed with more encroachment will have greater inputs of CO_2 to the groundwater based on findings of previous studies, which indicate that woody plant roots penetrate more deeply into the subsurface and thus can increase the downward transport of CO_2 (Wen et al., 2021).

We tested this hypothesis at Konza Prairie Biological Station (hereafter referred to as Konza Prairie), where long-term monitoring of stream water and groundwater in one of the watersheds (N4d) has demonstrated a significant increase in concentrations of CO_2 and mineral weathering products since the early 1990's (Macpherson et al., 2019; Macpherson et al., 2008; Macpherson and Sullivan, 2019a). Over that same time period, extensive woody encroachment has also occurred in watershed N4d (Dodds et al., 2023; Ratajczak et al., 2014) and thus woody encroachment may be a driver of the observed changes in groundwater chemistry. Climate change is also potentially a contributor (Vero et al., 2018). Mean annual precipitation and temperature have both increased at Konza Prairie over the past several decades (Keen et al., 2024; Sadayappan et al., 2023) and both changes favor increased CO_2 production by soil respiration (Davidson and Janssens, 2006; Fairbairn et al., 2023).

To build on these previous studies and better understand the impacts of woody encroachment, this study compares results from watershed N4d to results from an adjacent watershed, N1b, which has newly installed wells and considerably less woody encroachment. During the 2022 water year, we collected groundwater and stream samples approximately every three weeks to analyze variation in the bulk chemistry of water from each watershed. The study watersheds are adjacent to one another (Fig. 1), underlain by identical bedrock units, contain uniform assemblages of plant species, and are both grazed year-

round by bison. However, the watersheds differ in fire frequency, causing differences in the extents of woody encroachment in each. Woody plants cover about 28 % and 74 % of the upland and riparian areas, respectively, in watershed N4d, which is burned every four years, and about 6 % and 45 % of the upland and riparian areas, respectively, in watershed N1b, which is burned annually (Dodds et al., 2023). Thus, comparison of results between the watersheds provides the opportunity to examine impacts of woody encroachment outside of major differences in climate, bedrock composition, plant species assemblage, and grazing.

2. Study area

Konza Prairie is located in the Flint Hills region of eastern Kansas (Fig. 1). Since 1977, Konza Prairie has been divided into watersheds with different management practices in terms of fire frequency, fire season, and grazing. Watershed N4d (39.087356 N, 96.584417 W) has an area of 135.5 ha and is burned in the spring every four years whereas watershed N1b (39.08656 N, 96.57703 W) has an area of 118.8 ha and is burned every spring, creating differences in the extent of woody encroachment they contain, as noted above. Neither watershed has been cultivated and both have been grazed with American bison (*Bison bison*) since 1992.

Warm season grasses are dominant in each watershed and include big bluestem (*Andropogon gerardii*), little bluestem (*Schizachyrium scoparium*), Indian grass (*Sorghastrum nutans*), and switchgrass (*Panicum virgatum*) (Keen et al., 2022). Woody vegetation includes American elm (*Ulmus americana*), honey locust (*Gleditsia triacanthos*), bur oak (*Quercus macrocarpa*), chinquapin oak (*Quercus muehlenbergii*), hackberry (*Celtis occidentalis*), and redbud (*Cercis canadensis*), as well as smooth sumac (*Rhus glabra*), American plum (*Prunus americana*), and the clonal shrub species roughleaf dogwood (*Cornus drummondii*) (Keen et al., 2022).

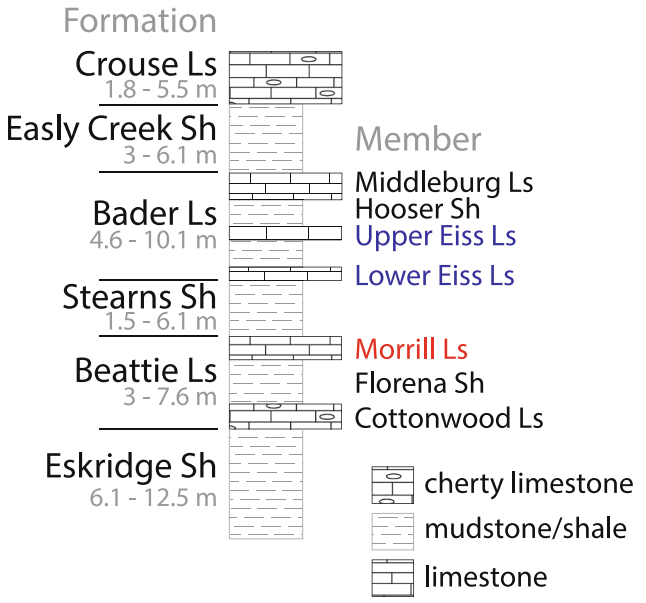

Fig. 2. Bedrock units that crop out approximately within the lower two-thirds of the study watersheds. Wells used in this study are screened within the Upper Eiss Limestone Member and the Lower Eiss Limestone Member of the Bader Formation and the Morrill Limestone Member of the Beattie Formation, Council Grove Group, Permian System. Limestone and shale are abbreviated Ls and Sh, respectively, and unit thickness ranges are shown in gray beneath each unit name. This stratigraphic column is based on Fig. 2a of Macpherson (1996) and modified from Hatley et al. (2023).

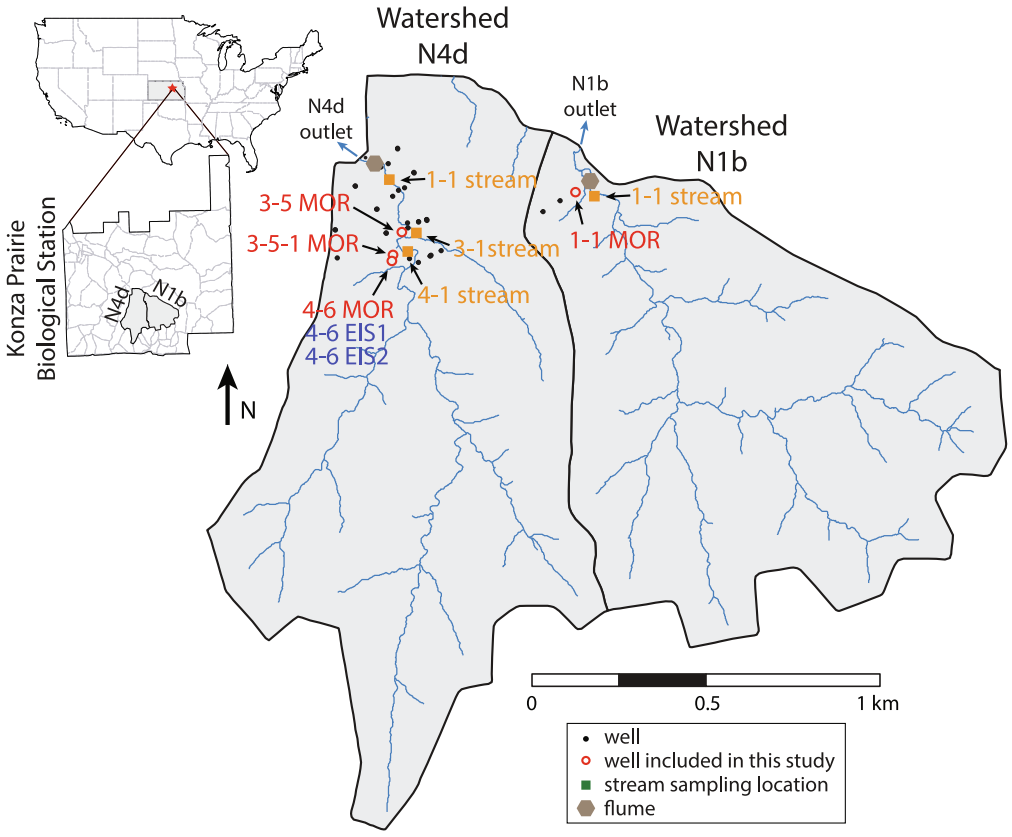

Fig. 1. Location of sampling sites within watersheds N4d and N1b at Konza Prairie Biological Station. Some well markers represent multiple wells within close proximity to one another.

Historically, woody vegetation has been largely confined to riparian areas, but shrub growth has increased along watershed hillslopes during recent decades (Briggs et al., 2005; Ratajczak et al., 2014).

Soils at Konza Prairie are predominantly silty-clay loams (Ransom et al., 1998), with thicknesses ranging from <20 to 50 cm in upland areas and up to about 2 m downslope (Sullivan et al., 2020). Underlying bedrock is Permian in age and consists of alternating units of horizontal limestone and mudrock (Fig. 2). Limestone units are 1–2 m thick, relatively permeable, and primarily composed of calcite with traces of dolomite (Macpherson et al., 2008), whereas the mudrocks are 2–4 m thick, have low permeability, and are primarily composed of illite, chlorite, and mixed-layer clays of chlorite-illite and chlorite-vermiculite (Macpherson and Sullivan, 2019a). The alternating nature of these bedrock units together with differences in rock mechanical properties gives each watershed a bench and slope topography, with limestone layers forming benches and weathered mudrocks forming slopes (Oviatt, 1998). The watersheds contain about 60 m of relief with slope gradients up to about 25 % (Sullivan et al., 2020).

The oldest bedrock unit in the watersheds is the Cottonwood Limestone (abbreviated Ls), which outcrops just downstream of the triangle-fluted stream gauging station at the outlet of watershed N4d (Fig. 1). The next two units above the Cottonwood Ls are the Morrill Ls and the Eiss Ls, with the Eiss informally divided into an upper and lower unit. Morrill and Eiss limestone units crop out in the lower fourth of the watersheds and have 31 wells completed within them in watershed N4d and five within watershed N1b. The wells are sealed with PVC caps when not in use and consist of 5 cm diameter PVC and have 61 cm long screens with gravel packs and bentonite seals (Macpherson, 1996). Above the Eiss Ls, four additional limestone and mudrock units are present, though no wells are completed within them.

Vertical groundwater flow between bedrock units is somewhat restricted by the low permeability of the mudrocks, with each limestone forming a semi-isolated aquifer connected by vertical leakage across mudrock units (Hatley et al., 2023; Macpherson, 1996). Groundwater flow within the limestone units primarily occurs within fractures and solution-enlarged pores, likely giving them highly heterogeneous hydraulic conductivities (Hatley et al., 2023). Accordingly, well productivity varies considerably from site to site, even for wells completed within the same unit (Macpherson, 1996). Furthermore, landscape position also appears to influence well productivity, with most of the wells in upland areas yielding little groundwater. Anhold (2023) estimated groundwater residence time in three Morrill Ls wells and one Upper Eiss Ls well based on sulfur hexafluoride concentrations measured in samples collected four times over the course of the 2022 water year. Results for each well varied with time and ranged from 2 to 31 years for the Morrill Ls (avg. 13 years) and 2 to 10 years for the Upper Eiss Ls (avg. 6 years), with no clear relationship to watershed encroachment or location.

Streamflow within each watershed is fed primarily by groundwater discharge from limestone layers that outcrop within the stream channel and along hillslopes (Hatley et al., 2023; Keen et al., 2022). Hatley et al. (2023) used end-member mixing analysis to show that less than 5 % of the streamflow analyzed during their study period (spring-summer 2021) was contributed by surface runoff and soil water in watershed N4d. The remainder was groundwater discharge from limestone units, which became fully connected to the stream after some threshold of groundwater storage was reached. Based on samples from the same time period, Swenson et al. (2024) found that much of the stream flow in the study area, potentially as high as 63 % at times, consisted of 'young water' that precipitated within 3 months and that the proportion of young water decreased as the stream dried. Taken together with results from Anhold (2023) and Hatley et al. (2023), the findings suggest groundwater age at the study area has a bimodal distribution, with a sizeable young fraction that turns over annually in well-connected conduits and an older fraction in relatively low permeability storage zones.

Mean annual precipitation and temperature are 811 mm and 11.7 °C, respectively (1983–2020; Sadayappan et al., 2023). However, much of the precipitation that falls (~75 %) is consumed by evapotranspiration (O'Keefe et al., 2020), and as such, the streams in each watershed are harshly intermittent. Stream flow at the outlet gauge stations of each watershed generally peaks from May to June and no flow is common from July through March each year (Costigan et al., 2015). Despite the lack of continuous flow most of the year, isolated pools persist year-round in places along each stream where groundwater discharges from limestone units (Macpherson, 1996; Swenson et al., 2024).

3. Methods

3.1. Sampling

To evaluate differences in groundwater and stream composition between the watersheds, we collected water samples for bulk chemical analysis and water stable isotopes roughly every three weeks from Oct. 31, 2021 to Oct. 30, 2022, which roughly coincides with the 2022 water year (Oct. 1 through Sept. 30). We collected stream samples just upstream of the flume at the outlet of each watershed (1–1 stream; Fig. 1). In addition, we collected stream samples at two sites in watershed N4d where groundwater discharges from the Eiss Ls and maintains a flowing pool within the stream channel (3–1 and 4–1 stream; Fig. 1). Stream flow was present at the sites near the flume only during five sampling trips for N1b and six for N4d during the study period, whereas water was present at the N4d 3–1 and 4–1 stream sites during every trip.

We collected groundwater samples for bulk chemical analysis from five wells in watershed N4d and one well in N1B. Although four additional wells are present in N1b, they rarely contain sufficient water for sampling, possibly reflecting their landscape position or whether their screens intersect flow conduits. We recognize that this sampling distribution limits our ability to characterize groundwater composition in N1b relative to N4d. However, we do have stream compositions at the outlets of each watershed, which integrate inputs from bedrock units upstream. Section 4.6 contains additional details about this limitation of our study.

To collect samples, we measured the depth to water (DTW) and total depth (TD) of each well using a Solinst water level meter and the bailed each well until the saturated volume of water had been removed at least two times, consistent with long term monitoring practices at the site (Kirk and Macpherson, 2024). Once the wells were purged, we collected a bail of water for chemical analysis and added a bottom emptying device to the bailer before discharging the samples in order to minimize gas exchanges. We filtered the samples with 0.45 μm syringe filters and then placed them into sample storage bottles. We stored samples in HDPE bottles for alkalinity and major cation and anion analyses and used glass vials for water isotope samples.

While collecting both the stream and groundwater samples, we measured the pH, temperature, dissolved oxygen (DO) concentration, and conductivity using Oakton PC 450 pH and conductivity probes and a Professional Series YSI Pro 2030 DO probe. We calibrated each probe before use and rinsed them with deionized water between sampling sites.

3.2. Laboratory analysis

We analyzed alkalinity and major ion concentrations for all samples within a month of collection in the Geology Department at Kansas State University. For alkalinity measurements, we used two techniques. During samples collected from Oct. 31, 2021 to Feb. 27, 2022, we used Gran alkalinity titrations with a glass burette and 0.02 N sulfuric acid titrant. Then, for the remainder of the samples, we used end-point (pH 4.5) titrations using a ThermoScientific OrionStarT910 pH Titrator again with 0.02 N sulfuric acid titrant. These methods gave consistent results when performed on replicate samples.

We measured anion (F^-, Cl^-, NO_3^-, SO_4^{2-}) and cation concentrations

(Na^+, K^+, Mg^{2+}, Ca^{2+}, Sr^{2+}) using Thermo Scientific ICS-1100 Ion Chromatographs. Quality control procedures included requiring a correlation coefficient of at least 0.995 for successful calibration and periodic analysis of calibration verification samples during each run. Precision and detection limits for these analyses are available in the online supplementary information (Table S1).

We measured the δ18O and δD of water isotope samples at 0.1 and 0.5 ‰ precision, respectively, using a Picarro L-i2130 water analyzer in the Stable Isotope Mass Spectrometry Laboratory at the Kansas State University Division of Biology. Results are expressed in delta notation relative to Vienna Standard Mean Ocean Water (VSMOW).

3.3. Statistical calculations and geochemical modeling

To evaluate the strength of differences between individual datasets, we used GraphPad Prism (v 6) software and conducted pairwise two-tailed Mann-Whitney tests, avoiding the assumption that our data are normally distributed. We also used GraphPad Prism to create box plots, with whiskers and outliers defined according to the Tukey method. Specifically, outliers are values that exceed the value of the 75th percentile plus 1.5 times the interquartile range (IQR) or values that fall below the value of the 25th percentile minus 1.5 times the IQR. Outliers are plotted as individual values and whiskers extend to the maximum and minimum values within the dataset that are not categorized as outliers.

We used the GSS module of the Geochemist's Workbench software (v 17) to calculate dissolved CO_2 concentrations, charge imbalance errors, and saturation indices for calcite and dolomite. For all geochemical modeling calculations, we used the default thermodynamic database used by the software (thermo.tdat; Delany and Lundeen, 1990) and the B-dot model for activities (Helgeson, 1969). The calculations were constrained by measured values for field parameters (pH, temperature, dissolved oxygen concentration), alkalinity, and concentrations of anions and cations. To limit potential impacts of analytical error on our analysis, we discarded alkalinity and major ion data for two samples that had excessive charge imbalance (20220416_N4d_3–5-1 Mor, 28.6 %; 20211221_N4d_4–6 Eis1, −16.48 %). Charge balance for all other samples ranged from −9.5 to 5.9 %, with an average imbalance of −2.7 %.

Lastly, we simulated mineral weathering in the study area using a two-stage kinetic reaction-path model created with the React module of The Geochemist's Workbench. The first stage simulates open-system calcite weathering by fixing the CO_2 fugacity of the system at the median partial pressure measured by Tsypin and Macpherson (2012) in watershed N4d (log $PCO_2 = -1.39$ atm). The second stage picks up the results from the first stage at various time points, representing different soil water residence times, and then continues calcite weathering until the solution reaches equilibrium but without fixed CO_2 fugacity. Here, the system is closed with respect to CO_2 and thus dissolved CO_2 concentration decreases as calcite weathers according to reaction 2. Stage one is intended to represent open-system weathering in soil whereas stage two represents closed-system weathering within underlying carbonate aquifers. For both stages, we assumed a temperature of 14.2 °C, consistent with the average groundwater temperature we measured during the 2022 water year. Moreover, we calculated calcite dissolution kinetics as described by Morse and Arvidson (2002), assuming conservative values for initial calcite abundance (10 mmol) and surface area (200 cm^2/g). Calcite abundance and surface area likely varies with depth below the surface. We lack data necessary to describe such variation and thus made no attempt to represent it within the model. As such, the rates of mineral weathering and soil water residence times should be taken as rough estimates. A detailed description of the model, including the script, is available in the Supplementary Information (Detailed Methods).

4. Results and discussion

The overall goal of this study was to answer the question: how do groundwater and stream CO_2 concentrations vary between watersheds with different extents of woody encroachment? We expected that the watershed with more encroachment would have higher dissolved CO_2 levels. However, our results indicate our hypothesis was incorrect. Below we describe and analyze our geochemical results and propose hypotheses that explain impacts of woody encroachment on CO_2 concentrations and bedrock weathering by altering soil CO_2 levels and soil water residence times. We then consider the implications of these findings for grasslands experiencing woody encroachment.

4.1. Variation in groundwater and surface water composition

The results of our water chemistry analyses represent the fundamental results on which our analysis is constructed. These results reveal differences in water chemistry between watersheds that provide clues about impacts of encroachment on CO_2 concentrations and mineral weathering. Our complete dataset is available online (Kirk and Macpherson, 2024). Here we focus on temperature, pH, dissolved oxygen, and major products of carbonate mineral weathering (calcium, magnesium, and alkalinity). Results for those parameters are shown in box plots in Fig. 3 and time series plots in the online supplementary information (Fig. S1). Table 1 lists summary statistics for all sampling locations.

In both watersheds, groundwater temperatures were similar for all wells and generally less variable than surface water temperatures (Fig. 3A; Table 1), which varied with surface conditions during the study period (Fig. S1). Among the wells sampled, groundwater temperature was most variable in N4d wells 4–6 Mor and 3–5 Mor, likely in response to the two-way interactions between groundwater and stream water that have been identified at those wells using dye tracers and geochemistry (Barry, 2018; Hatley et al., 2023; Macpherson, 1996).

Similarly, dissolved oxygen concentrations (O_2(aq)) did not vary consistently between watersheds. Dissolved oxygen concentrations in groundwater were mostly lower than surface water in both watersheds (Fig. 3B, Table 1), reflecting the ability of surface waters to exchange oxygen with the atmosphere and host phototrophic organisms. Among wells sampled, dissolved oxygen was lowest in N4d well 3–5-1 Mor, potentially reflecting a longer residence time of groundwater produced by that well compared to other wells in the study area (Anhold, 2023). Among the remaining wells, dissolved oxygen concentrations in Morrill Ls wells from both watersheds were similar and generally higher than those measured in groundwater from the overlying Eiss Ls.

Unlike temperature and dissolved oxygen concentration, groundwater and surface water pH did differ consistently between the more (N4d) and less (N1b) encroached watersheds. Average stream water pH was lower on average at the outlet of N1b (N1b 1–1 stream) than the outlet of N4d (N4d 1–1 stream) (Fig. 3C, Table 1). Similarly, groundwater pH was lower on average in N1b (N1b 1–1 Mor) than that for all of the N4d wells screened in the Morrill Ls and the Lower Eiss Ls (4–6 Eis1) and almost identical to the average for the N4d Upper Eiss Ls well (4–6 Eis2).

Concentrations of calcium, magnesium, and alkalinity in stream water were similar at the outlets of each watershed (Fig. 3D, E, F, Table 1). Outlet stream water in the less encroached watershed (N1b) had slightly greater calcium (N1b 1–1 stream) and alkalinity and lower magnesium than outlet stream water in the more encroached watershed (N4d 1–1 stream). The same pattern also holds for groundwater in each watershed. Samples from N1b 1–1 Mor had greater calcium and alkalinity content and lower magnesium content on average than all of the N4d wells screened in the Morrill Ls and both the lower Eiss Ls and upper Eiss Ls.

Water stable isotope compositions differed little between watersheds or between sample types (Fig. 4A, B, Table 1). The similarity between

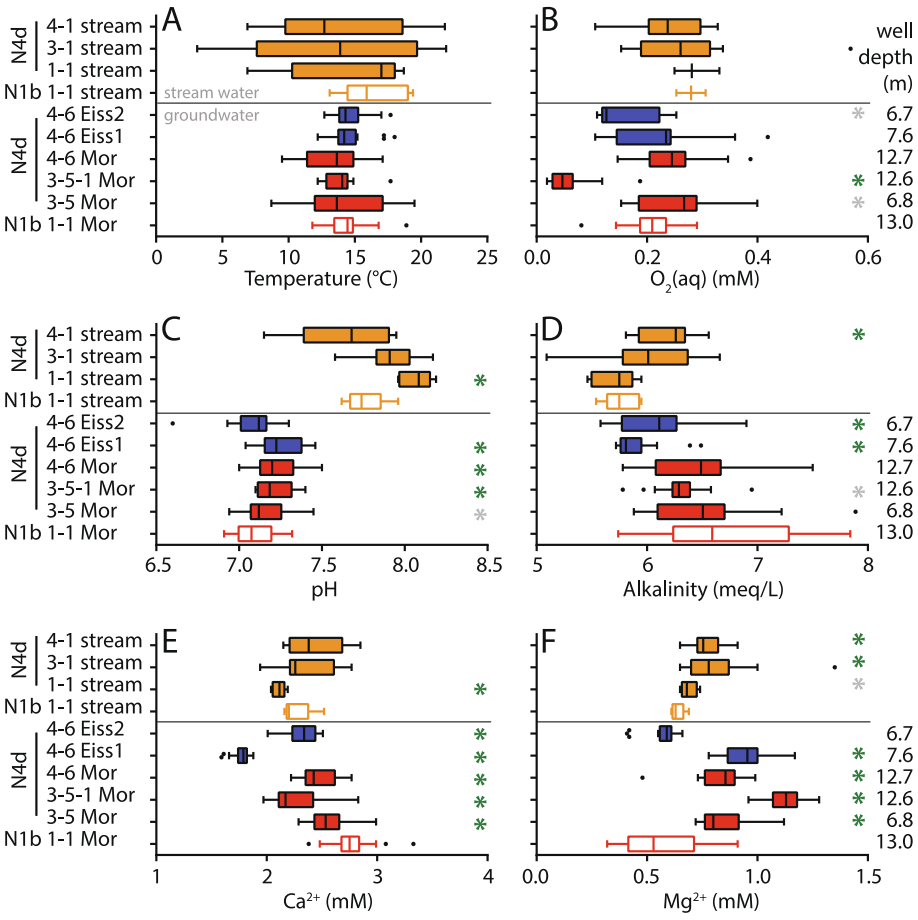

Fig. 3. Box plots showing variation in the (A) temperature, (B) dissolved oxygen concentration (O_2(aq)), (C) pH, and concentrations of (D) alkalinity, (E) calcium (Ca^{2+}), and (D) magnesium (Mg^{2+}) in surface water and groundwater samples. Total depths are indicated for each well along the right side of the figure. Box colors correspond to aquifer and sample type, with unfilled boxes used for N1b results and filled boxes for N4d results. Whiskers and outliers are defined according to the Tukey method (Section 3.3), with outliers plotted as individual scatter points. Asterisks on the right of each plot indicate *P* values calculated from Mann-Whitney tests that compare results for N4d samples to those for corresponding sample types from N1b. Specifically, groundwater data from N4d are compared to N1b 1–1 Mor and surface water data from N4d are compared to N1b 1–1 stream. A gray asterisk next to the N4d data indicates $P < 0.10$ difference from the corresponding N1b dataset and a green asterisk indicates $P < 0.01$. (For interpretation of the references to colour in this figure legend, the reader is referred to the web version of this article.)

Table 1
Water chemistry summary statistics.

	T	pH	O_2(aq)	Ca^{2+}	Mg^{2+}	Alkalinity	δD H_2O	$\delta^{18}O$ H_2O
	°C		mM	mM	mM	meq/L	‰ V-SMOW	‰ V-SMOW
	avg. (SD*)	avg. (SD)	avg. (SD)	avg. (SD)	avg. (SD)	avg. (SD)	avg. (SD)	avg. (SD)
Surface water								
N4d 4–1 stream	14.09 (5.09)	7.63 (0.27)	7.71 (2.21)	2.44 (0.25)	0.77 (0.08)	6.17 (0.23)	−35.21 (0.58)	−5.58 (0.17)
N4d 3–1 stream	12.93 (6.81)	7.91 (0.17)	8.81 (3.81)	2.37 (0.25)	0.82 (0.17)	5.99 (0.45)	−34.50 (1.29)	−5.41 (0.34)
N4d 1–1 stream	14.80 (4.67)	8.07 (0.09)	9.20 (1.31)	2.11 (0.06)	0.69 (0.04)	5.71 (0.19)	−34.83 (0.41)	−5.45 (0.22)
N1b 1–1 stream	16.56 (2.51)	7.76 (0.12)	8.95 (1.20)	2.26 (0.15)	0.64 (0.03)	5.78 (0.16)	−35.00 (0.71)	−5.54 (0.29)
Groundwater								
N4d 4–6 Eiss2	14.61 (1.33)	7.08 (0.16)	5.03 (1.74)	2.33 (0.14)	0.57 (0.08)	6.09 (0.37)	−35.53 (0.83)	−5.57 (0.26)
N4d 4–6 Eiss1	14.61 (1.61)	7.25 (0.13)	7.16 (2.95)	1.77 (0.09)	0.95 (0.10)	5.91 (0.24)	−36.87 (0.64)	−5.74 (0.17)
N4d 4–6 Mor	13.46 (2.28)	7.23 (0.14)	7.88 (2.23)	2.47 (0.17)	0.83 (0.12)	6.50 (0.49)	−35.33 (0.62)	−5.56 (0.18)
N4d 3–5-1 Mor	13.93 (1.32)	7.22 (0.11)	1.95 (1.53)	2.25 (0.22)	1.12 (0.08)	6.30 (0.27)	−37.00 (0.53)	−5.81 (0.11)
N4d 3–5 Mor	14.16 (3.17)	7.16 (0.14)	8.38 (2.46)	2.55 (0.18)	0.84 (0.11)	6.52 (0.53)	−35.07 (0.73)	−5.56 (0.14)
N1b 1–1 Mor	14.41 (1.68)	7.09 (0.12)	6.46 (1.74)	2.78 (0.23)	0.56 (0.18)	6.73 (0.61)	−35.67 (0.98)	−5.57 (0.22)

* SD = standard deviation

groundwater and surface water isotope ratios is consistent with previous studies that identified groundwater as the dominant streamflow source in the study area (Hatley et al., 2023; Keen et al., 2022). Values for both surface water and groundwater fall between average values for precipitation in April, September, and October defined by Keen et al. (2024) based on isotope data from precipitation samples collected weekly from 2001 through 2022. One potential explanation for these results is that groundwater recharge in both watersheds is biased toward

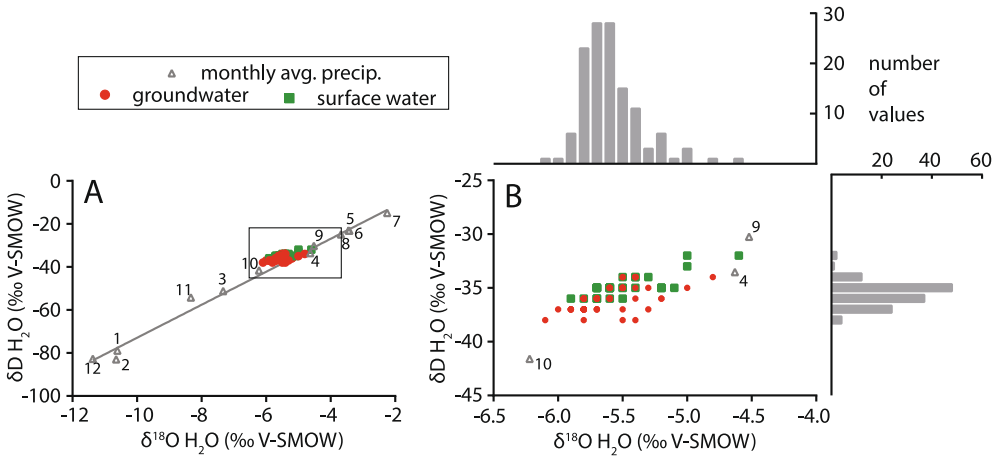

Fig. 4. Variation in the stable isotope composition of surface water (green) and groundwater (red) samples compared to the average monthly precipitation composition (gray; Keen et al., 2024). (A) Comparison of the data to monthly averages for precipitation from Keen et al. (2024), with numbers identifying which month each average represents and the line consisting of a best fit to the monthly averages. Graph (B) shows results from the inset box in (A). Results from 116 groundwater and 39 surface water samples are shown though results were identical for several samples and thus histograms are provided adjacent to the axes of (B) to show the distribution of values. (For interpretation of the references to colour in this figure legend, the reader is referred to the web version of this article.)

inputs at the start (April) and end (September – October) of the growing season, when precipitation is relatively high but transpiration losses are relatively low. The result may also reflect mixing of inputs from spring and summer with winter recharge, which has low δD and $\delta^{18}O$ values (Fig. 4A).

4.2. Variation in CO_2 budgets between watersheds

Precipitation contains low concentrations of dissolved CO_2, reflecting equilibrium with the atmosphere (Drever, 1997; Herczeg and Edmunds, 2000). However, as fresh precipitation percolates into soil, its dissolved CO_2 content typically increases because CO_2 partial pressures in soil gas are generally much greater (10-100×) than those in the atmosphere (Drever, 1997; Macpherson, 2009) as a result of root respiration and microbial organic matter degradation. CO_2 that dissolves into soil water forms carbonic acid, which can then drive mineral weathering reactions in the subsurface. Woody encroachment has the potential to alter inputs of CO_2 into the subsurface by changing root respiration rates, inputs of root exudates and other organic materials to soil, and recharge amounts and flow rates (Leite et al., 2023; Sullivan et al., 2019b; Vero et al., 2018; Wen et al., 2021).

To evaluate how groundwater and surface water CO_2 concentrations vary between watersheds with different amounts of encroachment, we used our water chemistry results to calculate dissolved CO_2 budgets. In the subsections that follow, we describe our calculations and how their results compare to our hypotheses. Further below (Section 4.3), we propose hypotheses to explain our findings and the mechanism by which encroachment alters groundwater CO_2 levels and weathering.

4.2.1. CO_2 concentrations in groundwater and surface water samples

Based on our geochemical speciation calculations, dissolved CO_2 levels in stream samples (avg. 0.27 mM) were on average four times lower than those in groundwater (avg. 1.12 mM) (Fig. 5A). Within watershed N4d, stream CO_2 concentrations decrease along flow from the 4–1 site (avg. 0.43 mM) to the watershed outlet (N4d 1–1 stream; avg. 0.12 mM), a trend that is consistent with previous CO_2 flux measurements in N4d (Norwood et al., 2023). Because groundwater discharge is the main source of stream flow (Hatley et al., 2023; Keen et al., 2022), the results indicate that CO_2 outgasses along flow after discharge of CO_2-rich groundwater into the stream channels, which explains the higher pH of stream water than groundwater (Fig. 3C) (Hatley et al., 2023; Norwood et al., 2023; Ohmes et al., 2009).

Between watersheds, CO_2 levels tended to be higher in the less encroached watershed (N1b) compared to the more encroached watershed (N4d). Average stream water CO_2 concentration at the outlet of N1b (N1b 1–1 stream; avg. 0.25 mM) was more than double that for the outlet stream water at N4d (N4d 1–1 stream; avg. 0.12 mM). Moreover, groundwater CO_2 concentrations were higher in N1b (N1b 1–1 Mor; avg.

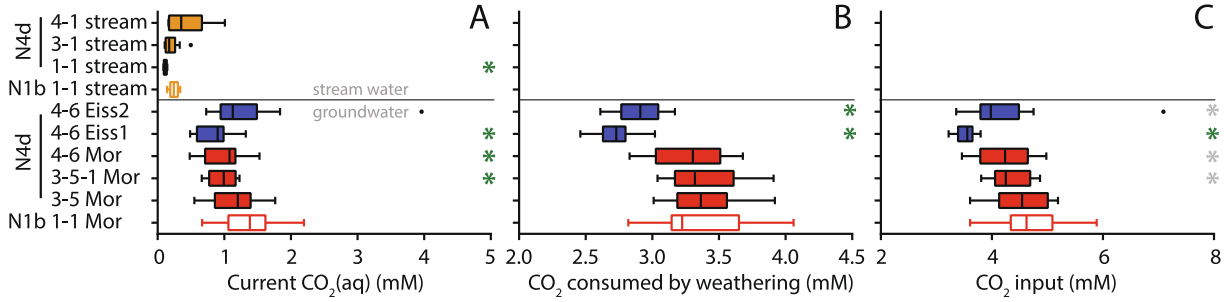

Fig. 5. CO_2 budget calculation results. Plot (A) shows variation in CO_2 concentrations calculated from geochemical speciation modeling, (B) shows the amounts of CO_2 consumed by carbonate mineral weathering, and (C) depicts our estimate of the amounts of CO_2 added per liter of recharge. Consistent with Fig. 3, a gray asterisk next to the N4d data indicates $P < 0.10$ difference from the corresponding N1b dataset and a green asterisk indicates $P < 0.01$. Full results of our geochemical speciation calculations are available in the online supplementary information (Table S2). (For interpretation of the references to colour in this figure legend, the reader is referred to the web version of this article.)

1.38 mM) than all of the N4d wells screened in the Morrill Ls (avg. 1.04 mM) and the Lower Eiss Ls (4–6 Eiss1; avg. 0.86 mM) and nearly identical to the average for the N4d Upper Eiss Ls well (4–6 Eiss2; 1.35 mM). Thus, differences in dissolved CO_2 between watersheds are largely inconsistent with our initial hypothesis that CO_2 levels would be higher in water in the more encroached watershed (N4d) than the less encroached watershed (N1b).

Groundwater CO_2(aq) concentrations we calculated (Fig. 5A) may underestimate actual levels in the aquifer if some CO_2(g) loss occurred during sampling. Consistent with this possibility, speciation calculations indicate that calcite and dolomite were slightly supersaturated in our groundwater samples (Fig. S2). CO_2(g) loss can drive carbonate minerals to supersaturation by increasing a solution's pH. If we assume that CO_2(g) loss caused calcite supersaturation and that the groundwater was actually equilibrated, we estimate that CO_2(aq) levels would be 0.45 mM and 0.90 mM higher on average in Eiss Ls and Morrill Ls groundwater (Fig. S3), respectively, compared to the values described above (Fig. 5A). Despite these increases, however, differences in CO_2(aq) concentrations remained the same between watersheds, with higher levels in the less encroached (N1b) than the more encroached watershed (N4d) (Fig. S3). Details about these calculations are available in the Supplementary Information (Detailed Methods).

In addition to CO_2(g) loss, other factors may also contribute to supersaturation of carbonate minerals in our groundwater samples. The equilibrium constants used in saturation index calculations may not be a perfect match with minerals in the study area (Bethke, 2022), which are likely unpure and vary in properties between units. A second possibility is that some particulate carbonate mass was small enough to pass through 0.45 μm filters used during sampling, which could have then dissolved when the samples were acidified (Bethke, 2022; Reed et al., 2022). Given the above considerations, in subsequent steps of our analysis, we used groundwater CO_2(aq) concentrations presented in Fig. 5A though we acknowledge that those values may have been impacted to some extent by outgassing.

4.2.2. CO_2 consumed by carbonate weathering

The main mineral weathering sink for soil CO_2 in the subsurface of the study area is carbonate weathering (Macpherson et al., 2008). Here, we use a simple inverse model to estimate the amount of CO_2 that would have been consumed by carbonate weathering per liter of groundwater. We excluded surface water from these calculations to avoid potential impacts of carbonate precipitation, which may accompany CO_2 outgassing from stream channels. Indeed, calcium, magnesium, and alkalinity levels decrease slightly in N4d stream water as it flows downstream from the 4–1 stream location to the watershed outlet (1–1 stream) (Fig. 3D, E, F, Table 1), consistent with carbonate precipitation along flow.

To estimate the amount of CO_2 consumed per liter of groundwater, we considered two weathering models. For the first model, we assumed CO_2 was consumed by reaction with both dolomite ($CaMg(CaCO_3)_2$) and calcite ($CaCO_3$), which can be described as follows:

$$CaMg(CO_3)_2 + 2\,CO_2(aq) + 2\,H_2O \leftrightarrow Ca^{2+} + Mg^{2+} + 4\,HCO_3^- \quad (1)$$

$$CaCO_3 + CO_2(aq) + H_2O \leftrightarrow Ca^{2+} + 2\,HCO_3^- \quad (2)$$

The reactions generate calcium and magnesium ions and thus we can use concentrations of those ions to estimate their net CO_2 consumption. Both calcite and dolomite were generally supersaturated in groundwater samples based on our geochemical results (Fig. S2), as noted above. However, little dolomite is present in the bedrock of the study area (Macpherson and Sullivan, 2019a). Instead, the magnesium in the groundwater may originate from ion exchange within the mudrocks that separate limestone units (Macpherson and Sullivan, 2019a):

$$Mg - clay + Ca^{2+} \leftrightarrow Ca - clay + Mg^{2+} \quad (3)$$

Therefore, for our second model, we assumed that ion exchange replaces some of the calcium generated by weathering with magnesium. We then estimated the number of moles of calcite consumed per liter of groundwater as the molar sum of calcium and magnesium concentrations.

Although dolomite is not abundant, both of these reaction pathways may be occurring to some extent. Regardless, both approaches give identical results in terms of estimated CO_2 consumption per liter of groundwater and the associated alkalinity production. Thus, our choice of which approach to use has no consequences for this study. Moreover, when we compare alkalinity production predicted by our models to concentrations we measured, we find reasonable agreement (Fig. S4). The root mean square error between measured alkalinity and predicted alkalinity (as bicarbonate) is only 0.51 meq/L, indicating that our calculations account well for the weathering history of our groundwater samples.

Results of these calculations indicate that weathering in Morrill Ls groundwater is insignificantly different between N1b and N4d, but it was significantly greater than the amount of weathering in the Eiss Ls (Fig. 5B). For Eiss Ls wells, average CO_2 consumption per liter of groundwater was 2.7 and 2.9 mmol for N4d 4–6 Eis1 and 4–6 Eis2, respectively. For Morrill Ls wells, average CO_2 consumption per liter of groundwater was 3.3 mmol for N1b 1–1 Mor compared to 3.4, 3.4, and 3.3 mmol for N4d 3–5 Mor, 3–5-1 Mor, and 4–6 Mor, respectively.

The lack of differences in weathering between watersheds was again inconsistent with our initial hypothesis. Moreover, the result seems contradictory to the higher CO_2 levels we observed in groundwater and surface water from the less encroached watershed (N1b) compared to the more encroached watershed (N4d). The result does not reflect a difference in the extent to which groundwater was able to equilibrate with the bedrock. As noted above, most samples we collected were slightly supersaturated with calcite and dolomite (Fig. S2). Instead, we hypothesize that the result stems from encroachment-driven changes the proportion of open-system weathering as well as potential changes in soil CO_2 levels, as discussed below (Section 4.3).

Lower amounts of weathering in groundwater from the Eiss Ls compared to the Morrill Ls may reflect variation in the properties of each unit and the sources of water they receive. Both units have similar but distinct compositions and hydrogeologic properties (Macpherson et al., 2019; Pomes, 1995; Wood and Macpherson, 2005), which may cause differences in their reactivities. The aquifers receive water from a network of bedrock fractures and do not necessarily interact with the stream in the same way (Barry, 2018; Gambill et al., 2024), potentially altering the concentrations and/or forms of weathering agents delivered to each. The Eiss Ls is stratigraphically higher than the Morrill Ls (Fig. 2) and preliminary evidence suggests that groundwater residence times range to higher values in the Morrill Ls compared to the Eiss Ls (Anhold, 2023), as described in Section 2. More work is needed to resolve variation in residence times in both aquifers, but longer residence times could contribute to greater weathering in the Morrill Ls than the Eiss Ls particularly for minerals that are less reactive than carbonates.

4.2.3. CO_2 added to recharge

If we assume that the dominant sink for CO_2 in the subsurface is mineral weathering and that CO_2 is supplied primarily from soil respiration, then the amount of CO_2 added per liter of recharge can be estimated as the sum of groundwater CO_2 concentrations and the amount consumed per liter by weathering. Microbial activity in the subsurface has the potential to add and remove CO_2 from the groundwater by catalyzing reactions that oxidize organic carbon, reduce CO_2 for catabolism or biosynthesis, or simply alter solution pH (Kirk, 2023). However, we reason that relatively low amounts of subsurface microbial activity occur over the relatively short residence time of groundwater in the aquifers (2–31 yr; Anhold, 2023), as evidenced by the elevated dissolved oxygen levels we measured in groundwater samples (Fig. 3B). Aquifer microorganisms preferentially respire oxygen before using electron

acceptors with lower reduction potentials such as nitrate, ferric iron, and sulfate (Bethke et al., 2011). Therefore, the fact that dissolved oxygen levels were largely elevated is evidence that aquifer microbial activity is limited.

Between watersheds, calculated CO_2 inputs tended to be slightly higher in the less encroached watershed (N1b) compared to the more encroached watershed (N4d) (Fig. 5C) mostly because of differences in current groundwater CO_2 concentrations (Fig. 5A). We estimate that Morrill Ls groundwater in N1b received 4.7 mmol of CO_2 per liter on average. In N4d, Morrill Ls groundwater received an average of 4.5, 4.3, and 4.2 mmol per liter for the 3–5 Mor, 3–5-1 Mor, and 4–6 Mor wells, respectively. Similarly, Eiss Ls groundwater in N4d received 4.2 and 3.5 mmol per liter in the 4–6 Eis2 and 4–6 Eis1 wells, respectively. CO_2 inputs to groundwater from N1b 1–1 Mor were greater with $P < 0.1$ than all of the wells in N4d other than 3–5 Mor.

4.3. Potential causes of differences in CO_2 concentrations between watersheds

The results of our CO_2 budget calculations were contrary to our initial hypotheses. We expected to find higher CO_2(aq) concentrations in the more encroached watershed (N4d) compared to the less encroached watershed (N1b), but we found the opposite. If these differences are representative of each watershed and not an artifact of data limitations, then we interpret that they are caused by woody encroachment, given that the watersheds experience the same climate, contain the same bedrock, and have the same grazing management. We reason that woody encroachment may be causing differences in CO_2(aq) concentrations by (1) changing soil CO_2 production and/or venting to the atmosphere, (2) decreasing soil water residence times, and/or (3) shifting the timing of groundwater recharge. In this section, we discuss these possibilities and compare them to our findings and those of previous studies.

CO_2(aq) concentrations may simply be lower in the more encroached watershed (N4d) than the less encroached watershed (N1b) because soil CO_2 generation is lower in N4d or because a greater fraction is emitted directly to the atmosphere in response to vegetative changes and/or increases in soil permeability. Both differences could lower the partial pressures of CO_2(g) in encroached soils and thus the CO_2(aq) concentration in soil and recharge water. Consistent with this possibility, Briggs et al. (2005) reported a 22 % higher annual CO_2 efflux from grassy soils compared to soils under an island of roughleaf dogwood at Konza Prairie. However, if encroachment lowered soil CO_2(g) levels, we would expect lower mineral weathering in the more encroached watershed (N4d) than the less encroached watershed (N1b), which is inconsistent with our findings (Fig. 5B). Moreover, other studies from diverse environments have found higher soil CO_2 generation associated with woody plants compared to grasses including Baldocchi et al. (2006), who studied an oak-grass savanna in California, USA, McCulley et al. (2004), who compared woodlands to remnant grasslands in subtropical Rio Grande Plains of southern Texas and northern Mexico, and Nghalipo and Throop (2021), who examined bare, grassy, and shub-dominated soils at a savanna in central Namibia. Thus, we conclude that encroachment-driven changes in soil CO_2 levels may contribute to differences we observed between watersheds, but that additional research is needed to evaluate this possibility.

Secondly, woody encroachment may be creating differences in CO_2(aq) concentrations by altering soil water residence times, which in turn affect the proportion of open- and closed-system mineral weathering in soils and the subsurface. It is well established that the outcome of carbonate weathering on groundwater CO_2 levels depends on the extent to which the system is open or closed to exchange of CO_2 gas (Drever, 1997; Freeze and Cherry, 1979). If dissolved CO_2 is not replenished from an adjacent gas phase as it is consumed by weathering (i.e., closed-system), then the dissolved CO_2 concentrations decrease as weathering occurs. In contrast, if dissolved CO_2 is replenished by a gas phase as weathering occurs (i.e., open-system), then CO_2 concentrations remain elevated as weathering progresses.

In the context of our study area, we interpret that soil respiration is the main source of CO_2 (Section 4.2.3). Bedrock fragments are abundant in Konza Prairie soils (Ransom et al., 1998), making it likely that reaction between CO_2 and bedrock minerals begins while recharge water is in the soil, as has been observed in other carbonate terrains (e.g., Williams et al., 2007). Within that unsaturated pore space, CO_2 that is consumed by weathering has the potential to be replaced by CO_2 in the soil gas, consistent with open-system weathering (Romero-Mujalli et al., 2019). However, as the water moves below the soil into the underlying bedrock, where we expect CO_2 production to be much lower (Section 4.2.3) and pores to be increasingly saturated (Sullivan et al., 2020), any additional mineral weathering would likely draw down CO_2 concentrations. Because woody encroachment increases soil infiltrability (Leite et al., 2020; Sullivan et al., 2019b), it increases the rate at which water can drain through the soil and thus decreases soil water residence time as recently demonstrated in the study area (Jarecke et al., 2024). As such, woody encroachment has the potential to decrease the amount of open-system weathering that can occur as water moves belowground and along groundwater flowpaths. This change would shift weathering downward because the water would have less time to equilibrate with bedrock fragments in the soil. Thus, the impact would be consistent with previous studies that concluded that encroachment increases bedrock weathering (Leite et al., 2020; Sullivan et al., 2019b; Wen et al., 2021). Moreover, this change would also result in lower groundwater CO_2 concentrations in more encroached watersheds, consistent with our results. We further examine this mechanism in Section 4.4 below.

Lastly, recharge timing could vary with encroachment because vegetative cover is one of the main controls on recharge dynamics (Jasechko et al., 2014; Kim and Jackson, 2012). Indeed, recent findings by Keen et al. (2024) suggest that woody encroachment is causing a decrease in the proportion of growing-season precipitation available for recharge in the study area. Such changes may contribute to differences in CO_2(aq) between variably-encroached watersheds because soil CO_2(g) levels vary seasonally. In watershed N4d, Tsypin and Macpherson (2012) measured the highest CO_2(g) partial pressures during the summer when moisture was not limiting and the lowest levels in the winter. However, the lack of differences in stable water isotope compositions between watersheds (Fig. 4A, B, Table 1) provides evidence that recharge timing is similar for both. Thus, we conclude that encroachment-driven changes in recharge timing are unlikely to have caused observed differences in CO_2(aq) concentrations between watersheds.

4.4. Testing changes in the proportion of open-system weathering as a cause of variation in CO_2(aq)

To fully test the hypothesis that encroachment is decreasing the proportion of open-system weathering by lowering soil water residence times, we would need additional data, including measurements of soil water residence times, weathering rates, and solution and gas compositions at various depths from the soil surface into the bedrock in areas with differing levels of encroachment. These data are not presently available. However, we can use our existing results together with geochemical modeling calculations as a preliminary test.

For this purpose, we constructed a two-stage kinetic reaction-path model using the React module of The Geochemist's Workbench as described in the methods and Supplementary Information. Model results are consistent with our hypothesis that variation in the proportion of open-system weathering can cause differences in groundwater composition that are similar to those we observed between watersheds. As soil water residence time and the proportion of open-system weathering increases, the equilibrated groundwater concentrations of CO_2, calcium, and bicarbonate increase while pH decreases (Fig. 6A). For soil water residence times less than about 2 days, calcite weathering occurred

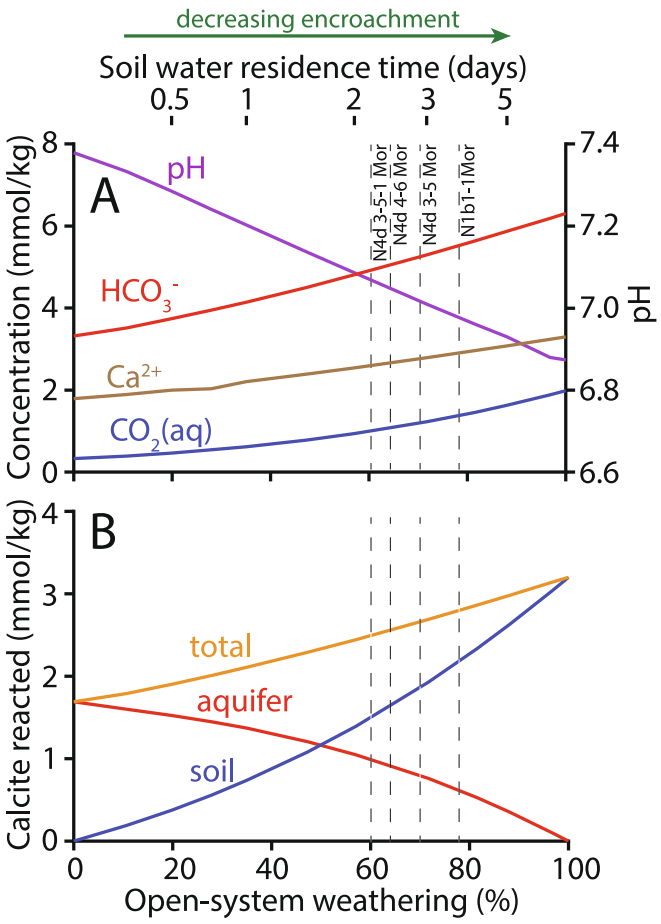

Fig. 6. Variation with the proportion of open-system weathering in (A) final (i.e., equilibrated) groundwater compositions and (B) weathering distribution calculated by the kinetic reaction-path model. Concentrations are normalized relative to kilograms of solvent water. Dashed vertical lines correspond to median concentrations of dissolved CO_2 calculated for Morrill Ls wells in both watersheds. The top of plot A shows rough estimates of soil water residence times associated with different proportions of open-system weathering.

primarily under closed system conditions in the aquifer (Fig. 6B) because the water is relatively far from equilibrium as it moves from the soil into the aquifer. Conversely, for soil water residence times greater than 2 days, calcite largely equilibrated under open-system conditions in the soil, thereby limiting aquifer weathering.

Vertical dashed lines in Fig. 6 correspond to median concentrations of dissolved CO_2 calculated for Morrill Ls wells in both watersheds. pH values and calcium concentrations intersected by those lines indicate that the model slightly underestimated pH and alkalinity and overestimated calcium concentrations relative to median values from samples collected during the study period. These differences likely reflect the simplicity of the weathering model, which does not account for variation in bedrock mineralogy, ion exchange reactions, or many chemical and biological reactions that can alter solution pH and alkalinity content. Nonetheless, the reaction-path model does provide proof of concept for our interpretation and some insight into differences between watersheds. Based on the model results and median dissolved CO_2 concentrations we determined for Morrill Ls groundwater, the proportion of open-system weathering ranged from about 60 to 70 % for watershed N4d and was nearly 80 % for watershed N1b (Fig. 6). These values correspond to soil water residence times of about 2 to 3 days for N4d and nearly 4 days for N1b according to the rate law used for the reaction-path model. Alongside these shifts, the model predicts a substantial change in the depth of weathering. Aquifer weathering accounts for 30 to 40 % of the total calcite weathering in N4d based on median CO_2 concentrations and about 22 % of the weathering in N1b.

Lastly, some discussion of the total amount of weathering calculated by the model is warranted. Based on median CO_2 concentrations we determined for Morrill Ls wells, the amount of calcite weathering predicted by the model was 2.5 to 2.7 mmol per kilogram of solvent water for N4d and 2.8 mmol per kilogram for N1b (Fig. 6B). In contrast, the values calculated directly from groundwater composition were 3.3 to 3.4 mmol per liter for N4d and 3.2 mmol per liter for N1b (Fig. 5), noting that a liter of dilute groundwater has a water mass of about 1 kg. Thus, our model underestimates the amounts of weathering that occurred.

Numerous factors have the potential to contribute to this difference. The difference may reflect the simplicity of our model, which does not simulate all of the phenomena that alter groundwater compositions at the study area, as noted above. The difference may reflect some degassing of CO_2 during sampling, as discussed in Section 4.2.1. Our assumption of closed-system weathering in the aquifer and open-system weathering in the soil is likely not uniformly met. Electrical resistivity imaging in watershed N4d is consistent with greater pore saturation in the bedrock compared to the overlying soils (Sullivan et al., 2020). As such, the results indicate a greater likelihood of open-system weathering in study area soils compared to the bedrock. However, bedrock water saturation is spatially variable likely as a result of bedrock heterogeneity (Sullivan et al., 2020). Our model does not capture the diverse mineral species that likely weather in the study area, which include carbonate and silicate minerals from the bedrock as well dust inputs (Macpherson and Sullivan, 2019b). Moreover, the choice of CO_2 partial pressure and/or temperature for the model is also an important consideration, given that both are major controls on amounts of calcite weathering (Covington et al., 2023; Romero-Mujalli et al., 2019; Sullivan et al., 2019a) and have the potential to differ between watersheds.

Although we did not observe differences in the total amount of weathering between watersheds as indicated by the model, we did find on average lower calcium and alkalinity concentrations in groundwater from N4d than N1b (Fig. 3D, E). The results suggest, therefore, that weathering rates may be lower in N4d than N1b at times during the year, as expected if a higher proportion of open-system weathering occurs in N1b. Moreover, it is worth noting that, although woody encroachment has progressed more in watershed N4d than N1b, both watersheds are still dominated by grasses. Changes in the amount of weathering between watersheds may become more apparent if the extent of woody encroachment in each continues to diverge in the years ahead.

4.5. Implications

Our analysis indicates that the physical impact of woody encroachment can extend deep in the subsurface, beyond the depth of woody roots, by shortening soil water residence time and thereby shifting weathering downward. By altering bedrock porosity and permeability, deeper weathering associated with encroachment would alter the ability of bedrock to store groundwater and transmit it to adjacent streams, as suggested previously (Sadayappan et al., 2023; Sullivan et al., 2019b; Vero et al., 2018). Moreover, we reason that this impact of encroachment may be greater in systems with carbonate bedrock, such as the study area, compared to those with siliciclastic or crystalline bedrock, given that carbonate minerals tend to react on shorter timescales than silicates (Sullivan et al., 2019a). As such, bedrock composition may influence the extent to which woody plant removal is an effective strategy for recovering streamflow in encroached watersheds (e.g., Bosch and Hewlett, 1982; Dodds et al., 2023; Dugas et al., 1998; Wilcox et al., 2006). Woody plant removal can increase catchment water budgets by reducing transpiration losses from woody plants, but it would not reverse encroachment-driven changes to bedrock porosity and permeability.

A second implication of our findings is that woody encroachment can impact the pathway and amount of soil CO_2 that reaches the

atmosphere. CO_2 generated in soils can be emitted directly to the atmosphere, and more work is needed to constrain this loss of CO_2(g) from study area soils. However, a considerable fraction can also be transported into the subsurface with recharge water (Sanchez-Canete et al., 2018). As soil CO_2 makes its way through the subsurface, it can be consumed by mineral and microbial reactions, potentially trapping it's carbon as dissolved ions, biomass, and carbonate minerals (Kirk, 2023; Kirk et al., 2013). If the groundwater ultimately discharges into an aquatic habitat at the surface, some portion of the remaining CO_2 can then be lost from the solution if its concentration exceeds the level set by equilibrium with the atmosphere (Butman and Raymond, 2011; Duvert et al., 2018). Our findings imply that woody encroachment can decrease the proportion of soil CO_2 that is transported into the subsurface. As a result, woody encroachment would also lower the likelihood that soil CO_2 could be trapped in the subsurface by chemical and microbial reactions.

Lastly, a third implication is that woody encroachment is not causing the increase in groundwater CO_2 inputs over time observed at Konza Prairie by Macpherson et al. (2019), Macpherson et al., 2008). Our results suggest that groundwater CO_2 concentrations would actually be higher in the absence of woody encroachment. Instead, the increase may be driven by the increases in temperature and precipitation that have occurred over the past several decades at the study area (Keen et al., 2024; Macpherson et al., 2008; Sadayappan et al., 2023) or perhaps other factors.

4.6. Limitations and future steps

One of the main limitations of this study is the limited access to groundwater in watershed N1b. We only included results for one well in N1b because the four other wells are generally dry or nearly so. In contrast, we have results for three Morrill Ls wells and two Eiss Ls wells in N4d. We recognize that this uneven sampling distribution limits our ability to characterize groundwater composition in N1b relative to N4d. However, we did include stream compositions at the outlets of each watershed, and streams integrate geochemical signatures of entire watersheds above their sampling sites (Manning et al., 2020). The differences we observed in stream outlet composition are consistent with differences in groundwater sample compositions between watersheds, indicating that groundwater CO_2 concentrations are higher overall in the less encroached (N1b) compared to the more encroached (N4d) watershed.

Differences in stream water CO_2(aq) concentrations between watersheds may reflect differences in the extent to which the water has equilibrated with the atmosphere as it has flowed downstream. Fluxes of CO_2(g) from high-order stream water are characterized by high spatial heterogeneity, reflecting variation in CO_2 and groundwater inputs and the ability of the water to exchange CO_2 with the atmosphere (Duvert et al., 2018; Marx et al., 2017). However, the stream CO_2(aq) concentrations we compare in our analysis were collected at uniform landscape positions in each watershed (1–1 stream, Fig. 1), suggesting that the stream water at those locations has flowed over the same stratigraphic units and had similar opportunities for gas exchanges. Moreover, when we effectively add lost CO_2(g) back to the stream water using the approach discussed in Section 4.2.1, differences in CO_2(aq) concentration persist between watersheds, with higher concentrations in the less encroached (N1b) than the more encroached watershed (N4d). Thus, we reason that have a solid basis for comparing stream CO_2(aq) concentrations, though we acknowledge that potential differences in stream water gas exchanges add uncertainty to the comparison.

Lastly, as noted above, we currently lack data to fully test the hypotheses described in Section 4.3. However, our analysis can provide a framework to guide future investigations to better understand the belowground consequences of woody encroachment. According to our findings, more data are needed to assess impacts of encroachment on soil CO_2(g) partial pressures at the watershed scale. Doing so is challenging, given the heterogeneous nature of soils (Cable et al., 2012), though the data would greatly advance our understanding of the biogeochemical and hydrologic consequences of woody encroachment. Data are needed to further evaluate the extent to which bedrock weathering is closed with respect to CO_2(g) exchange. Moreover, additional data are needed to constrain weathering kinetics, including measurements of soil water residence times, groundwater flow rates, mineral abundances and surface areas, and solution compositions at various depths from the soil into the bedrock.

5. Concluding remarks

We used periodic sampling of groundwater and surface water during the 2022 water year to evaluate impacts of encroachment on water chemistry and mineral weathering in two adjacent grassland watersheds, one containing 6 % and 45 % woody plant coverage in upland and riparian areas (watershed N1b), respectively, and the other containing 28 % and 74 % (watershed N4d), respectively. We hypothesized that CO_2 inputs to shallow groundwater and amounts of mineral weathering would increase with the extent of woody encroachment. However, our results indicate that CO_2 inputs were actually higher in the less encroached (N1b) than the more encroached watershed (N4d) and amounts of mineral weathering per liter of groundwater were insignificantly different. We hypothesize that woody encroachment caused differences in CO_2(aq) concentrations between watersheds by decreasing soil water residence time, which in turn decreased the extent to which mineral weathering occurred under conditions that are open with respect to CO_2 gas exchange. This possibility is consistent with our field data and geochemical modeling calculations and implies that impacts of encroachment extend deep into the subsurface, creating a stronger weathering engine at depth, and that encroachment alters the amount and pathways by which soil CO_2 can reach the atmosphere. In addition to altering soil water residence times, encroachment may also be altering CO_2(aq) concentrations in the watersheds by changing soil CO_2 production and/or venting. Our analysis indicates that future research that determines soil CO_2 levels at the watershed scale, constraints on mineral reaction kinetics, and the extent to which closed-system weathering occurs with depth in the subsurface would further advance our understanding of the biogeochemical and hydrologic impacts of woody encroachment in grasslands.

CRediT authorship contribution statement

Christa Anhold: Writing – review & editing, Writing – original draft, Visualization, Resources, Methodology, Investigation, Formal analysis, Data curation, Conceptualization. **Camden Hatley:** Writing – review & editing, Methodology, Investigation. **Eresay Alcantar-Velasquez:** Writing – review & editing, Investigation. **Rachel M. Keen:** Writing – review & editing. **Kayalvizhi Sadayappan:** Writing – review & editing. **Karla M. Jarecke:** Writing – review & editing. **Pamela L. Sullivan:** Writing – review & editing, Funding acquisition, Conceptualization. **Jesse B. Nippert:** Writing – review & editing, Funding acquisition, Conceptualization. **Li Li:** Writing – review & editing. **G.L. Macpherson:** Writing – review & editing, Methodology. **Matthew F. Kirk:** Writing – review & editing, Writing – original draft, Visualization, Supervision, Resources, Project administration, Methodology, Funding acquisition, Formal analysis, Data curation, Conceptualization.

Declaration of competing interest

The authors declare the following financial interests/personal relationships which may be considered as potential competing interests.

Matthew Kirk reports financial support was provided by National Science Foundation. If there are other authors, they declare that they have no known competing financial interests or personal relationships that could have appeared to influence the work reported in this paper.

Acknowledgements

We acknowledge that research on Konza Prairie uses land taken from those who lived here before us, including the Kaw/Kansa, Osage, and Pawnee and hope that our work honors their existence and those of their ancestors who remain. We thank three anonymous reviewers who provided helpful feedback on our manuscript as well as the many researchers, technicians, and volunteers who manage Konza Prairie Biological Station. This project was supported with funding from the US National Science Foundation's Long Term Ecological Research program (DEB-2025849).

Appendix A. Supplementary data

Supplementary data to this article can be found online at https://doi.org/10.1016/j.chemgeo.2024.122522.

Data availability

Data used for this study are available online via the KNZ Data Catalog, dataset AGW01, as cited in the text. Results of calculations using those data are available in the supplementary information.

References

Acharya, B., Kharel, G., Zou, C., Wilcox, B., Halihan, T., 2018. Woody Plant Encroachment Impacts on Groundwater Recharge: a Review. Water 10, 1–26. https://doi.org/10.3390/w10101466.

Anhold, C., 2023. Impacts of Woody Encroachment on the Fate of Soil CO2 in a Grassland Watershed (MS Thesis). Kansas State University, Manhattan, Kansas, USA.

Baldocchi, D., Tang, J., Xu, L., 2006. How switches and lags in biophysical regulators affect spatial-temporal variation of soil respiration in an oak-grass savanna. J. Geophys. Res. Biogeosci. 111. https://doi.org/10.1029/2005JG000063.

Barger, N.N., Archer, S.R., Campbell, J.L., Huang, C., Morton, J.A., Knapp, A.K., 2011. Woody plant proliferation in north American drylands: a synthesis of impacts on ecosystem carbon balance. J. Geophys. Res. Biogeosci. 116. https://doi.org/10.1029/2010JG001506.

Barry, E.R., 2018. Characterizing Groundwater Flow through Merokarst, Northeast Kansas, USA (MS Thesis). University of Kansas, Lawrence, KS.

Bethke, C.M., 2022. Geochemical and Biogeochemical Reaction Modeling, third. ed. Cambridge University Press, New York.

Bethke, C.M., Sanford, R.A., Kirk, M.F., Jin, Q., Flynn, T.M., 2011. The thermodynamic ladder in geomicrobiology. Am. J. Sci. 311, 183–210. https://doi.org/10.2475/03.2011.01.

Bosch, J.M., Hewlett, J.D., 1982. A review of catchment experiments to determine the effect of vegetation changes on water yield and evapotranspiration. J. Hydrol. 55, 3–23. https://doi.org/10.1016/0022-1694(82)90117-2.

Brantley, S.L., Eissenstat, D.M., Marshall, J.A., Godsey, S.E., Balogh-Brunstad, Z., Karwan, D.L., Papuga, S.A., Roering, J., Dawson, T.E., Evaristo, J., Chadwick, O., McDonnell, J.J., Weathers, K.C., 2017. Reviews and syntheses: on the roles trees play in building \hack\newline and plumbing the critical zone. Biogeosciences 14, 5115–5142. https://doi.org/10.5194/bg-14-5115-2017.

Briggs, J.M., Knapp, A.K., Blair, J.M., Heisler, J.L., Hoch, G.A., Lett, M.S., McCarron, J.K., 2005. An ecosystem in transition. Causes and consequences of the conversion of Mesic grassland to shrubland. Biogeosci 55, 243–254. https://doi.org/10.1641/0006-3568(2005)055[0243:aeitca]2.0.co;2.

Brunsell, N.A., Van Vleck, E.S., Nosshi, M., Ratajczak, Z., Nippert, J.B., 2017. Assessing the Roles of Fire Frequency and Precipitation in determining Woody Plant expansion in Central U.S. Grasslands. J. Geophys. Res. Biogeosci. 122, 2683–2698. https://doi.org/10.1002/2017JG004046.

Butman, D., Raymond, P.A., 2011. Significant efflux of carbon dioxide from streams and rivers in the United States. Nat. Geosci. 4, 839–842. https://doi.org/10.1038/NGEO1294.

Cable, J.M., Barron-Gafford, G.A., Ogle, K., Pavao-Zuckerman, M., Scott, R.L., Williams, D.G., Huxman, T.E., 2012. Shrub encroachment alters sensitivity of soil respiration to temperature and moisture. J. Geophys. Res. Biogeosci. 117. https://doi.org/10.1029/2011JG001757.

Canadell, J., Jackson, R.B., Ehleringer, J.B., Mooney, H.A., Sala, O.E., Schulze, E.-D., 1996. Maximum rooting depth of vegetation types at the global scale. Oecologia 108, 583–595. https://doi.org/10.1007/BF00329030.

Collins, S.L., Nippert, J.B., Blair, J.M., Briggs, J.M., Blackmore, P., Ratajczak, Z., 2021. Fire frequency, state change and hysteresis in tallgrass prairie. Ecol. Lett. 24, 636–647. https://doi.org/10.1111/ele.13676.

Costigan, K.H., Daniels, M.D., Dodds, W.K., 2015. Fundamental spatial and temporal disconnections in the hydrology of an intermittent prairie headwater network. J. Hydrodyn. 522, 305–316. https://doi.org/10.1016/j.jhydrol.2014.12.031.

Covington, M.D., Martin, J.B., Toran, L.E., Macalady, J.L., Sekhon, N., Sullivan, P.L., García Jr., Á.A., Heffernan, J.B., Graham, W.D., 2023. Carbonates in the critical Zone. Earth's Future 11, e2022EF002765. https://doi.org/10.1029/2022EF002765.

Davidson, E.A., Janssens, I.A., 2006. Temperature sensitivity of soil carbon decomposition and feedbacks to climate change. Nature 440, 165–173. https://doi.org/10.1038/nature04514.

Delany, J.M., Lundeen, S.R., 1990. The LLNL Thermochemical Database. LLNL report UCRL-21658.. Lawrence Livermore National Laboratory.

Dodds, W.K., 1997. Distribution of Runoff and Rivers Related to Vegetative Characteristics, Latitude, and Slope: a Global Perspective. J. N. Am. Benthol. Soc. 16, 162–168. https://doi.org/10.2307/1468248.

Dodds, W.K., Robinson, C.T., Gaiser, E.E., Hansen, G.J.A., Powell, H., Smith, J.M., Morse, N.B., Johnson, S.L., Gregory, S.V., Bell, T., Kratz, T.K., McDowell, W.H., 2012. Surprises and Insights from Long-Term Aquatic Data Sets and experiments. BioScience 62, 709–721. https://doi.org/10.1525/bio.2012.62.8.4.

Dodds, W.K., Ratajczak, Z., Keen, R.M., Nippert, J.B., Grudzinski, B., Veach, A., Taylor, J. H., Kuhl, A., 2023. Trajectories and state changes of a grassland stream and riparian zone after a decade of woody vegetation removal. Ecol. Appl., e2830 https://doi.org/10.1002/eap.2830.

Drever, J.I., 1997. The Geochemistry of Natural Waters. Prentice Hall, Upper Saddle River, NJ.

Dugas, W.A., Hicks, R.A., Wright, P., 1998. Effect of removal of Juniperus ashei on evapotranspiration and runoff in the Seco Creek Watershed. Water Resour. Res. 34, 1499–1506. https://doi.org/10.1029/98WR00556.

Duvert, C., Butman, D.E., Marx, A., Ribolzi, O., Hutley, L.B., 2018. CO2 evasion along streams driven by groundwater inputs and geomorphic controls. Nat. Geosci. 11. https://doi.org/10.1038/s41561-018-0245-y, 813-+.

Fairbairn, L., Rezanezhad, F., Gharasoo, M., Parsons, C.T., Macrae, M.L., Slowinski, S., Van Cappellen, P., 2023. Relationship between soil CO2 fluxes and soil moisture: Anaerobic sources explain fluxes at high water content. Geoderma 434, 116493. https://doi.org/10.1016/j.geoderma.2023.116493.

Freeze, R.A., Cherry, J.A., 1979. Groundwater. Prentice-Hall, Inc, Englewood Cliffs, NJ.

Gambill, I., Zipper, S., Kirk, M., Seybold, E., 2024. Exploring drivers of groundwater recharge at Konza Prairie (Flint Hills region, Kansas, USA) using transfer function noise models (Open-file Report no. 2024–6). Kansas Geological Survey, Lawrence, KS.

Hatley, C.M., Armijo, B., Andrews, K., Anhold, C., Nippert, J.B., Kirk, M.F., 2023. Intermittent streamflow generation in a merokarst headwater catchment. Environ. Sci.: Adv. https://doi.org/10.1039/D2VA00191H.

Helgeson, H.C., 1969. Thermodynamics of hydrothermal systems at elevated temperatures and pressures. Am. J. Sci. 267, 729–804.

Herczeg, A., Edmunds, W., 2000. Inorganic Ions as Tracers, pp. 31–77. https://doi.org/10.1007/978-1-4615-4557-6_2.

Hibbard, K.A., Archer, S., Schimel, D.S., Valentine, D.W., 2001. Biogeochemical changes accompanying woody plant encroachment in a subtropical savanna. Ecology 82, 1999–2011. https://doi.org/10.1890/0012-9658(2001)082[1999:BCAWPE]2.0.CO;2.

Huxman, T.E., Wilcox, B.P., Breshears, D.D., Scott, R.L., Snyder, K.A., Small, E.E., Hultine, K., Pockman, W.T., Jackson, R.B., 2005. Ecohydrological implications of woody plant encroachment. Ecology 86, 308–319. https://doi.org/10.1890/03-0583.

Jarecke, K.M., Zhang, X., Keen, R., Dumont, M., Li, B., Sadayappan, K., Moreno, V., Ajami, H., Billings, S.A., Flores, A., Hirmas, D., Kirk, M.F., Li, L., Nippert, J., Singha, K., Sullivan, P., 2024. Woody Encroachment Modifies Subsurface Structure and Hydrological Function. Ecohydrology. https://doi.org/10.1002/eco.2731.

Jasechko, S., Birks, S.J., Gleeson, T., Wada, Y., Fawcett, P.J., Sharp, Z.D., McDonnell, J. J., Welker, J.M., 2014. The pronounced seasonality of global groundwater recharge. Water Resour. Res. 50, 8845–8867. https://doi.org/10.1002/2014wr015809.

Keen, R.M., Nippert, J.B., Sullivan, P.L., Ratajczak, Z., Ritchey, B., O'Keefe, K., Dodds, W. K., 2022. Impacts of Riparian and Non-riparian Woody Encroachment on Tallgrass Prairie Ecohydrology. Ecosystems. https://doi.org/10.1007/s10021-022-00756-7.

Keen, R.M., Sadayappan, K., Jarecke, K.M., Li, L., Kirk, M.F., Sullivan, P.L., Nippert, J.B., 2024. Unexpected hydrologic response to ecosystem state change in tallgrass prairie. J. Hydrol. 643, 131937. https://doi.org/10.1016/j.jhydrol.2024.131937.

Kgope, B.S., Bond, W.J., Midgley, G.F., 2010. Growth responses of African savanna trees implicate atmospheric [CO2] as a driver of past and current changes in savanna tree cover. Austral Ecol. 35, 451–463. https://doi.org/10.1111/j.1442-9993.2009.02046.x.

Kim, J.H., Jackson, R.B., 2012. A Global Analysis of Groundwater Recharge for Vegetation, climate, and Soils. Vadose Zone J. 11. https://doi.org/10.2136/vzj2011.0021RA.

Kirk, M.F., 2023. Microbiology for Earth Scientists, 1st ed. New Prairie Press, Manhattan, KS.

Kirk, M.F., Macpherson, G.L., 2024. AGW01 long-term measurement of groundwater physical and chemical properties from wells on watershed N04D at Konza Prairie. KNZ Data Catalog. https://doi.org/10.6073/pasta/e63a877c079f4923f9cbfd2662ec2ff7.

Kirk, M.F., Santillan, E.F.U., Sanford, R.A., Altman, S.J., 2013. CO2-induced shift in microbial activity affects carbon trapping and water quality in anoxic bioreactors. Geochim. Cosmochim. Acta 122, 198–208. https://doi.org/10.1016/j.gca.2013.08.018.

Leite, P.A.M., Wilcox, B.P., McInnes, K.J., 2020. Woody plant encroachment enhances soil infiltrability of a semiarid karst savanna. Environ. Res. Communicati. 2, 115005. https://doi.org/10.1088/2515-7620/abc92f.

Leite, P.A.M., Schmidt, L.M., Rempe, D.M., Olariu, H.G., Walker, J.W., McInnes, K.J., Wilcox, B.P., 2023. Woody plant encroachment modifies carbonate bedrock: field

evidence for enhanced weathering and permeability. Sci. Rep. 13, 15431. https://doi.org/10.1038/s41598-023-42226-7.
Lu, J., Zhang, Q., Werner, A.D., Li, Y., Jiang, S., Tan, Z., 2020. Root-induced changes of soil hydraulic properties – a review. J. Hydrol. 589, 125203. https://doi.org/10.1016/j.jhydrol.2020.125203.
Macpherson, G.L., 1996. Hydrogeology of thin limestones: the Konza Prairie Long-Term Ecological Research Site, Northeastern Kansas. J. Hydrol. 186, 191–228. https://doi.org/10.1016/s0022-1694(96)03029-6.
Macpherson, G.L., 2009. CO2 distribution in groundwater and the impact of groundwater extraction on the global C cycle. Chem. Geol. 264, 328–336. https://doi.org/10.1016/j.chemgeo.2009.03.018.
Macpherson, G.L., Sullivan, P.L., 2019a. Watershed-scale chemical weathering in a merokarst terrain, northeastern Kansas, USA. Chem. Geol. 527. https://doi.org/10.1016/j.chemgeo.2018.12.001.
Macpherson, G.L., Sullivan, P.L., 2019b. Dust, impure calcite, and phytoliths: Modeled alternative sources of chemical weathering solutes in shallow groundwater. Chem. Geol. 527, 118871. https://doi.org/10.1016/j.chemgeo.2018.08.007.
Macpherson, G.L., Roberts, J.A., Blair, J.M., Townsend, M.A., Fowle, D.A., Beisner, K.R., 2008. Increasing shallow groundwater CO2 and limestone weathering, Konza Prairie, USA. Geochim. Cosmochim. Acta 72, 5581–5599. https://doi.org/10.1016/j.gca.2008.09.004.
Macpherson, G., Sullivan, P., Stotler, R., Norwood, B., 2019. Increasing groundwater CO2 in a mid-continent tallgrass prairie: Controlling factors. In: E3S Web of Conferences 98. https://doi.org/10.1051/e3sconf/20199806008.
Maher, K., 2010. The dependence of chemical weathering rates on fluid residence time. Earth Planet. Sci. Lett. 294, 101–110. https://doi.org/10.1016/j.epsl.2010.03.010.
Manning, A.H., Morrison, J.M., Wanty, R.B., Mills, C.T., 2020. Using stream-side groundwater discharge for geochemical exploration in mountainous terrain. J. Geochem. Explor. 209, 106415. https://doi.org/10.1016/j.gexplo.2019.106415.
Marx, A., Dusek, J., Jankovec, J., Sanda, M., Vogel, T., van Geldern, R., Hartmann, J., Barth, J.A.C., 2017. A review of CO2 and associated carbon dynamics in headwater streams: a global perspective. Rev. Geophys. 55, 560–585. https://doi.org/10.1002/2016RG000547.
McCarron, J.K., Knapp, A.K., Blair, J.M., 2003. Soil C and N responses to woody plant expansion in a Mesic grassland. Plant Soil 257, 183–192.
McCulley, R.L., Archer, S.R., Boutton, T.W., Hons, F.M., Zuberer, D.A., 2004. Soil respiration and nutrient cycling in wooded communities developing in grasslands. Ecology 85, 2804–2817. https://doi.org/10.1890/03-0645.
Morse, J.W., Arvidson, R.S., 2002. The dissolution kinetics of major sedimentary carbonate minerals. Earth Sci. Rev. 58, 51–84. https://doi.org/10.1016/S0012-8252(01)00083-6.
Nghalipo, E.N., Throop, H.L., 2021. Vegetation patch type has a greater influence on soil respiration than does fire history on soil respiration in an arid broadleaf savanna woodland, Central Namibia. J. Arid Environ. 193, 104577. https://doi.org/10.1016/j.jaridenv.2021.104577.
Nimmo, J.R., 2021. The processes of preferential flow in the unsaturated zone. Soil Sci. Soc. Am. J. 85, 1–27. https://doi.org/10.1002/saj2.20143.
Norwood, B.S., Stotler, R.L., Brookfield, A., Sullivan, P.L., Macpherson, G.L., 2023. Flux and stable isotope fractionation of CO2 in a Mesic prairie headwater stream. J. Water Clim. Change 14, 1961–1976. https://doi.org/10.2166/wcc.2023.067.
Ohmes, K.S., Macpherson, G., Huff, B.L., 2009. Low stream-flow measurement and stream CO2 emission calculation, Konza Prairie LTER site, Northeastern Kansas, USA. Geol. Soc. Am. Abstr. Programs 41, 664.
O'Keefe, K., Bell, D.M., McCulloh, K.A., Nippert, J.B., 2020. Bridging the Flux Gap: Sap Flow Measurements Reveal Species-specific patterns of Water Use in a Tallgrass Prairie. J. Geophys. Res. Biogeosci. 125, e2019JG005446. https://doi.org/10.1029/2019JG005446.
Oviatt, C.G., 1998. Geomorphology of Konza Prairie. In: Knapp, A.K., Briggs, J.M., Hartnett, D.C., Collins, S.L. (Eds.), Grassland Dynamics. Oxford University Press, New York, pp. 35–47.
Pawlik, Ł., Phillips, J.D., Šamonil, P., 2016. Roots, rock, and regolith: Biomechanical and biochemical weathering by trees and its impact on hillslopes—a critical literature review. Earth Sci. Rev. 159, 142–159. https://doi.org/10.1016/j.earscirev.2016.06.002.
Pomes, M.L., 1995. A Study of the Aquatic Humic Substances and Hydrogeology in a Prairie Watershed: Use of Humic Material as a Tracer of Recharge through Soils (Ph. D. thesis). University of Kansas, Lawrence, KS.
Qiao, L., Zou, C.B., Stebler, E., Will, R.E., 2017. Woody plant encroachment reduces annual runoff and shifts runoff mechanisms in the tallgrass prairie, USA. Water Resour. Res. 53, 4838–4849. https://doi.org/10.1002/2016WR019951.
Ransom, M., Rice, C.W., Todd, T.C., Wehmueller, W.A., 1998. Soils and soil biota. In: Knapp, A.K., Briggs, J.M., Hartnett, D.C., Collins, S.L. (Eds.), Grassland Dynamics. Oxford University Press, New York, pp. 48–66.
Ratajczak, Z., Nippert, J.B., Ocheltree, T.W., 2014. Abrupt transition of Mesic grassland to shrubland: evidence for thresholds, alternative attractors, and regime shifts. Ecology 95, 2633–2645.
Reed, M.H., Strope, E.K., Cremona, F., Myers, J.A., Newell, S.E., McCarthy, M.J., 2022. Effects of filtration timing and pore size on measured nutrient concentrations in environmental water samples. Limnol. Oceanogr. Methods. https://doi.org/10.1002/lom3.10529.
Romero-Mujalli, G., Hartmann, J., Börker, J., Gaillardet, J., Calmels, D., 2019. Ecosystem controlled soil-rock pCO2 and carbonate weathering – Constraints by temperature and soil water content. Chem. Geol. 527, 118634. https://doi.org/10.1016/j.chemgeo.2018.01.030.
Sadayappan, K., Keen, R., Jarecke, K.M., Moreno, V., Nippert, J.B., Kirk, M.F., Sullivan, P.L., Li, L., 2023. Drier streams despite a wetter climate in woody-encroached grasslands. J. Hydrol. 130388. https://doi.org/10.1016/j.jhydrol.2023.130388.
Sanchez-Canete, E.P., Barron-Gafford, G.A., Chorover, J., 2018. A considerable fraction of soil-respired CO2 is not emitted directly to the atmosphere. Sci. Rep. 8, 13518. https://doi.org/10.1038/s41598-018-29803-x.
Scott, R.L., Huxman, T.E., Williams, D.G., Goodrich, D.C., 2006. Ecohydrological impacts of woody-plant encroachment: seasonal patterns of water and carbon dioxide exchange within a semiarid riparian environment. Glob. Chang. Biol. 12, 311–324. https://doi.org/10.1111/j.1365-2486.2005.01093.x.
Silva, L.C.R., Anand, M., Oliveira, J.M., Pillar, V.D., 2009. Past century changes in Araucaria angustifolia (Bertol.) Kuntze water use efficiency and growth in forest and grassland ecosystems of southern Brazil: implications for forest expansion. Glob. Chang. Biol. 15, 2387–2396. https://doi.org/10.1111/j.1365-2486.2009.01859.x.
Stevens, N., Lehmann, C.E.R., Murphy, B.P., Durigan, G., 2017. Savanna woody encroachment is widespread across three continents. Glob. Chang. Biol. 23, 235–244. https://doi.org/10.1111/gcb.13409.
Sullivan, P.L., Macpherson, G.L., Martin, J.B., Price, R.M., 2019a. Evolution of carbonate and karst critical zones. Chem. Geol. 527, 119223. https://doi.org/10.1016/j.chemgeo.2019.06.023.
Sullivan, P.L., Stops, M.W., Macpherson, G.L., Li, L., Hirmas, D.R., Dodds, W.K., 2019b. How landscape heterogeneity governs stream water concentration-discharge behavior in carbonate terrains (Konza Prairie, USA). Chem. Geol. 527, 118989. https://doi.org/10.1016/j.chemgeo.2018.12.002.
Sullivan, P.L., Zhang, C., Behm, M., Zhang, F., Macpherson, G.L., 2020. Toward a new conceptual model for groundwater flow in merokarst systems: Insights from multiple geophysical approaches. Hydrol. Process. 34, 4697–4711. https://doi.org/10.1002/hyp.13898.
Swenson, L.J., Zipper, S., Peterson, D.M., Jones, C.N., Burgin, A.J., Seybold, E., Kirk, M.F., Hatley, C., 2024. Changes in Water Age during Dry-down of a Non-Perennial Stream. Water Resour. Res. 60, e2023WR034623. https://doi.org/10.1029/2023WR034623.
Tsypin, M., Macpherson, G.L., 2012. The effect of precipitation events on inorganic carbon in soil and shallow groundwater, Konza Prairie LTER Site, NE Kansas, USA. Appl. Geochem. 27, 2356–2369. https://doi.org/10.1016/j.apgeochem.2012.07.008.
Vero, S.E., Macpherson, G.L., Sullivan, P.L., Brookfield, A.E., Nippert, J.B., Kirk, M.F., Datta, S., Kempton, P., 2018. Developing a Conceptual Framework of Landscape and Hydrology on Tallgrass Prairie: a critical Zone Approach. Vadose Zone J. 17, 11.
Wang, J., Xiao, X., Zhang, Y., Qin, Y., Doughty, R.B., Wu, X., Bajgain, R., Du, L., 2018. Enhanced gross primary production and evapotranspiration in juniper-encroached grasslands. Glob. Chang. Biol. 24, 5655–5667. https://doi.org/10.1111/gcb.14441.
Watson, K.W., Luxmoore, R.J., 1986. Estimating Macroporosity in a Forest Watershed by use of a Tension Infiltrometer. Soil Sci. Soc. Am. J. 50, 578–582. https://doi.org/10.2136/sssaj1986.03615995005000030007x.
Wen, H., Sullivan, P.L., Macpherson, G.L., Billings, S.A., Li, L., 2021. Deepening roots can enhance carbonate weathering by amplifying CO_2-rich recharge. Biogeosciences 18, 55–75. https://doi.org/10.5194/bg-18-55-2021.
Wilcox, B.P., Owens, M.K., Dugas, W.A., Ueckert, D.N., Hart, C.R., 2006. Shrubs, streamflow, and the paradox of scale. Hydrol. Process. 20, 3245–3259. https://doi.org/10.1002/hyp.6330.
Wilcox, B.P., Basant, S., Olariu, H., Leite, P.A.M., 2022. Ecohydrological connectivity: a unifying framework for understanding how woody plant encroachment alters the water cycle in drylands. Front. Environ. Sci. 10.
Williams, E.L., Szramek, K.J., Jin, L., Ku, T.C.W., Walter, L.M., 2007. The carbonate system geochemistry of shallow groundwater–surface water systems in temperate glaciated watersheds (Michigan, USA): significance of open-system dolomite weathering. GSA Bull. 119, 515–528. https://doi.org/10.1130/B25967.1.
Wood, H.K., Macpherson, G.L., 2005. Sources of Sr and implications for weathering of limestone under tallgrass prairie, northeastern Kansas. Appl. Geochem. 20, 2325–2342. https://doi.org/10.1016/j.apgeochem.2005.08.002.
Xiao, D., Brantley, S.L., Li, L., 2021. Vertical Connectivity Regulates Water Transit Time and Chemical Weathering at the Hillslope Scale. Water Resour. Res. 57, e2020WR029207. https://doi.org/10.1029/2020WR029207.
Zou, C.B., Turton, D.J., Will, R.E., Engle, D.M., Fuhlendorf, S.D., 2014. Alteration of hydrological processes and streamflow with juniper (Juniperus virginiana) encroachment in a Mesic grassland catchment. Hydrol. Process. 28, 6173–6182. https://doi.org/10.1002/hyp.10102.
Zou, C.B., Caterina, G.L., Will, R.E., Stebler, E., Turton, D., 2015. Canopy Interception for a Tallgrass Prairie under Juniper Encroachment. PLoS One 10, e0141422. https://doi.org/10.1371/journal.pone.0141422.